Available online at www.eccomasproceedia.org
Eccomas Proceedia COMPDYN (2023) 432-456

ECCOMAS
Proceedia

COMPDYN 2023
9th ECCOMAS Thematic Conference on
Computational Methods in Structural Dynamics and Earthquake Engineering
M. Papadrakakis, M. Fragiadakis (eds.)
Athens, Greece, 12-14 June 2023

ALTERNATIVE RETROFIT STRATEGIES FOR SEISMIC RISK REDUCTION: STUDYING THE EFFECTIVENESS OF LOW-DAMAGE EXTERNAL EXOSKELETONS.

Simone D'Amore[1], **Livio Pedone**[1], **and Stefano Pampanin**[1]

[1] Sapienza University of Rome, Department of Structural and Geotechnical Engineering
Via Eudossiana 18, 00184, Rome, Italy
{simone.damore, livio.pedone, stefano.pampanin}@uniroma1.it

Abstract

Recent earthquakes occurred worldwide have further highlighted the high vulnerability of existing Reinforce Concrete RC buildings built prior the enforcement of modern seismic codes. For this reason, such buildings are generally expected to be 'earthquake prone'. As a result, in recent decades, an unprecedent research effort has been undertaken to develop efficient and cost-effective retrofit strategies able to improve safety, reduce the expected losses related to earthquake damage, and, in general terms, enhance the resilience of the existing building stock and the overall community. More specifically, both local retrofit interventions (e.g., based on the use of Fiber Reinforced Polymers, FRP, concrete or steel jacketing, etc.) as well as global ones (e.g., based on the use of shear walls or external exoskeletons) have been developed.
The main outcome of this work is to evaluate the effectiveness and thus support the attractiveness of low-damage exoskeletons when compared to other retrofit strategies. The low-damage technology herein considered is the PREcast Seismic Structural Systems (PRESSS) developed in the 1990's. In a first phase, a pre-1970 RC buildings has been selected as a case study building and assessed in terms of seismic performance considering both non-linear static (push-over) as well as more refined non-linear dynamic methods. Using results, the Safety-Index as well as the Expected Annual Losses (EAL) have been evaluated, and suggestions are provided to improve the simplified procedures currently available for the calculation of the latter index (EAL). Finally, alternative retrofit strategies have been implemented for the seismic retrofit of the as-built configuration, and the push-over based method has been used to calculate the Safety-Index as well as the Expected Annual Losses of the retrofitted configurations. The results of this work confirm the improved performance of low-damage exoskeletons when compared to similar traditional global strategies and even further when compared with local strategies.

Keywords: RC structures, Seismic Assessment, Seismic Retrofit, Low-Damage Exoskeletons, Seismic Loss Assessment, Fragility Analysis

ISSN:2623-3347
Peer-review under responsibility of the organizing committee of COMPDYN 2023.
doi: 10.7712/120123.10412.21292

1 INTRODUCTION

In last decades, the high seismic vulnerability of the European building stock built prior the 1970's, especially in the Mediterranean Area, has been further pointed out by recent severe earthquakes. Such buildings are generally not compliant with modern building codes, since they have been designed following an elastic approach based on "working stresses" and not considering "capacity design" (or "hierarchy of strength") principles.. This aspect generally led to poorly and inadequate details (e.g., use of low-quality materials, reduced or absent stirrups within the joint region, limited transverse reinforcement in structural members, use of plain round bars and end-hooked anchorages within the joints, inadequate development length and lap-splice generally located in the plastic hinge zone, poor diaphragm-to-lateral resisting system connection), which generally cause brittle failure mechanisms potentially leading to local/global collapse mechanisms [1].

For the reasons highlighted before, in recent years, research activities have assessed the need to develop efficient, yet cost-effective, strategies and techniques for the seismic retrofit of buildings. Among these, both local (i.e., mainly aiming at modifying the "hierarchy of strength" within beam-column subassemblies) as well as global retrofit solutions have been proposed.

Specifically, in recent years exoskeleton-type interventions have been growing in interest due to their advantage to be implemented entirely from outside the building, reducing as much as possible the occupants' disruption. Furthermore, such solution allows for an easy implementation of the integrated (i.e., seismic/energetic/architectural) renovation of buildings, allowing to move towards a more resilient - against natural hazard -, energy efficient and sustainable society. For these reasons, the implementation of efficient integrated (i.e. seismic and energetic) renovation strategies is nowadays particularly important in order to foster un unprecedent action to achieve an actual transition towards a low-carbon and eco-efficient society in line with the European targets for GreenHouse Gas (GHG) emissions reduction [2, 3].

In this perspective, the use of engineered exoskeleton (mainly used for the seismic upgrading), especially if implemented in the form of low-damage technology, (e.g., the PREcast Seismic Structural System, PRESSS [4, 5, 6]), can represent a valuable opportunity to develop an efficient integrated renovation strategy of the built environment. In fact, the exoskeleton can act as a support for a high-multi-performance "double-skin" of the building, allowing also for energetic and architectural upgrading. Nevertheless, recent earthquakes have pointed out the high vulnerability of non-structural components, which can lose functionality for low-intensity earthquakes and collapse for moderate-to-strong ones. For this reason, in recent years an unprecedent effort has been dedicated to the development of low-damage technologies both for structural as well as non-structural components [7, 8, 9]. Recently, the efficiency of integrated low-damage solutions has been proved by tri-dimensional shake table tests on a scaled two-story building prototype at LNEC laboratory in Lisbon [10, 11, 12]. Furthermore, recent earthquakes occurred in New Zealand have proved the high performances of low-damage (i.e., PRESSS) buildings [7]. In addition, low-damage technologies for masonry infill walls [13,14], interior dry-wall partitions [15], heavy claddings [16] and glazing systems [17] have been proposed.

Even though the energy efficiency and sustainability are topics of growing interests, this paper focuses only on the comparison among retrofit alternatives from a seismic point of view. More specifically, building on the definition of a Safety-Index (i.e., namely %NBS in the NZSEE 2017 guidelines, or IS-V in the Italian Seismic Classification Guidelines 2017, and defined as the ratio among the capacity of a building to the demand on a newly designed one on the same site, [18,19]), and of the Expected Annual Losses (i.e., EAL, or Perdite Annue Medie, PAM, in Italian [19]), a comparison among the proposed retrofit alternative strategies

defined in the following is presented. In particular, several methods have been used for the definition of the EAL, and a proposal for refinement of the simplified tool available in the [19] is also herein presented. Furthermore, considering only the as-built configuration in this preliminary work, both simplified yet accurate non-linear static (pushover) analyses, as well as more refined, yet more complex and time consuming, Non-Linear Time History Analyses (NLTHAs) have been used for the definition of IS-V and EAL.

2 REVIEW OF SAFETY EVALUATION AND LOSS ASSESSMENT PROCEDURES

A detailed assessment of the seismic performance of existing buildings is critical to support the definition and implementation of the most suitable retrofit strategies and techniques. In line with the Performance-Based Earthquake Engineering (PBEE) philosophy, the assessment phase should address both life safety and socio-economic consequences/losses (direct and indirect). Following this goal, Cornell et al., [20], proposed a probabilistic-based PBEE framework, later adopted by the Pacific Earthquake Engineering Research (PEER) Center. From a mathematical point of view, the PEER's PBEE framework aims to assess the frequency of exceeding various thresholds for a specific performance metric (decision variable, DV) of greatest interest to stakeholders (e.g., economic losses, casualties, and downtime). The procedure involves 4 distinct analysis steps, i.e. hazard, structural, damage, and loss analysis.

For the practical implementation of the probabilistic-based PEER's PBEE methodology, a supporting tool referred to as the Performance Assessment Calculation Tool (PACT), has been developed and provided together with the FEMA P-58 report [21]. More specifically, the methodology described in the FEMA P-58 report and implemented in the PACT tool is based on a building-specific component-based approach and allows for either an (i) intensity-based, (ii) scenario-based (e.g., Probable Maximum Loss, PML), or (iii) time-base (e.g., Expected Annual Loss, EAL) performance assessment evaluation. Nevertheless, the implementation of the fully probabilistic component-based PBEE methodology typically requires significant computational effort and high scientific background, making it potentially not suitable for engineering practice [22], or for stakeholders/end-users dealing with large buildings portfolios, such as (re)insurance company [23].

Therefore, significant research efforts have been carried out in the recent past to develop simplified, yet reliable, seismic loss assessment procedures for buildings. For instance, in order to reduce the computational effort of the structural analysis phase in the PEER's PBEE framework, Bianchi et al. [24] proposed an analytical procedure for the cost/performance-based evaluation of buildings, based on the SLaMA (Simple Lateral Mechanism Analysis, [18]) method. The same authors also carried out a cost/performance-based comparison between traditional and low-damage building systems by adopting a pushover-based methodology, [25]. In this work, non-linear static procedures were identified as the best compromise between simplicity and accuracy when compared to other simplified (linear static) or more refined (non-linear dynamic) structural analysis methods.

Yet, in probabilistic seismic risk assessment investigation on building portfolios, building-level fragility models are typically adopted, describing the probability of achieving or exceeding a specific damage state (DS) given a ground-motion intensity measure (IM); thus, vulnerability relationships are derived through a damage-to-loss model, describing the expected loss ratio (LR) for each considered DS (e.g., [26]). Martin and Silva [27] developed fragility and vulnerability models for the most common building classes at the global level by performing non-linear dynamic (time history) analyses (NLTHA) on equivalent single-degree-of-freedom (SDoF) systems. The proposed models account for both building-to-building and record-to-record variability. Similarly, Gentile and Galasso [28] proposed a simplified loss-assessment

framework, based on the derivation of building-level fragility and vulnerability curves. The proposed framework has been applied for the selection of the best retrofit strategy for existing RC buildings considering increasing levels of analysis methods: SLaMA, numerical pushover, and NLTHAs. The authors concluded that, when the proposed loss assessment methodology is implemented, the ranking of the different retrofit solutions can be deemed not-sensitive to the structural analysis method; therefore, these results would suggest adopting the non-linear static approaches for the preliminary retrofit design phase, where several alternative retrofit strategies could be considered. Nevertheless, the authors pointed out that, once the optimal retrofit strategy and technique are identified, more refined component-based assessment procedures (e.g., [21]) are recommended to evaluate the effective benefits of the selected retrofit intervention.

In this context, the Italian "Guidelines for seismic risk classification of constructions", also referred to as the "Sismabonus" guidelines [19,22], introduced a simplified methodology for the seismic-risk classification of existing buildings. Although this document deals with advanced metrics of the PBEE philosophy (e.g., EAL), the proposed procedure is deemed suitable for practical applications due to its simplicity, [22]. In this methodology, the seismic risk class of the analyzed structure is identified by estimating a Safety Index (IS-V, equivalent to the %New Building Standard, %NBS adopted by [18]) and an economic index EAL (or PAM, "Perdita Annua Media", in the Italian guidelines). For the implementation of the procedure, a non-linear static analysis is required, and the seismic performance of the structure at different Limit States (i.e., Operational, O-LS; Damage Limitation, DL-LS; Life Safety, LS-LS; and Collapse Prevention Limit State, CP-LS) is evaluated through a spectrum-based approach (e.g., the Capacity Spectrum Method, CSM, [29] or the N2 method, [30]), (Figure 1a). Thus, for each considered LS the equivalent Peak Ground Acceleration (PGA) capacity is assessed and the corresponding return period T_r is evaluated. Moreover, a direct economic loss expressed as the Reconstruction Cost percentage ($\%RC$, and equivalent to Loss Ratio, LR) is associated with each LS. In this way, it is possible to define a Mean Annual Frequency (MAF) of exceeding, $\lambda = 1/T_r$ vs %RC curve. The EAL value is then computed as the area underneath the λ–%RC curve (Figure 1b).

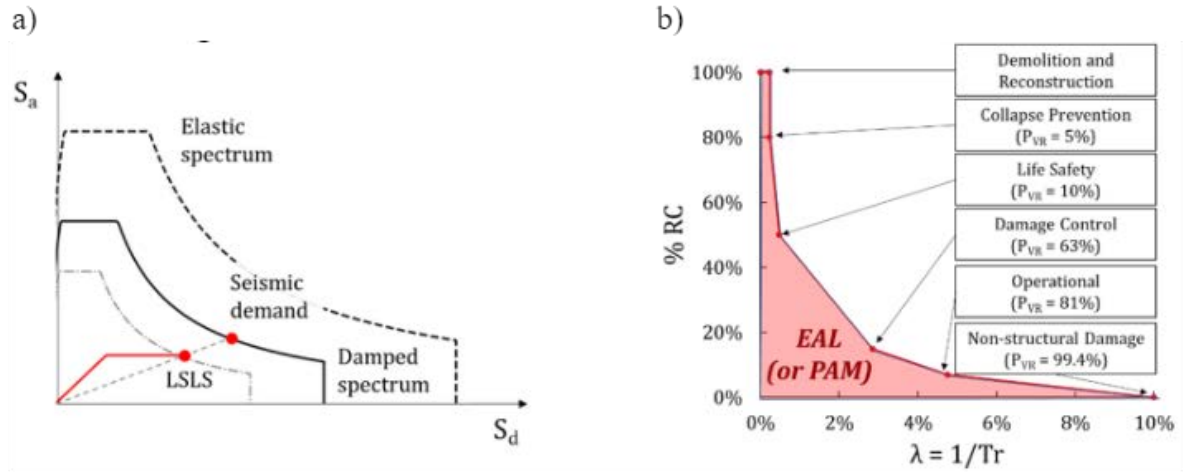

Figure 1: a) Capacity/Demand comparison at the LS-LS according to the Capacity Spectrum Method, and b) evaluation of the EAL index following the Italian "Sismabonus" guideline (after [19]).

Taking advantage of the simplicity of its procedure, the methodology introduced by the Italian "Sismabonus" guidelines can represent a valuable supporting tool for evaluating and classifying the seismic risk of existing buildings. However, some limitations with respect to more-refined loss-assessment analyses can be identified, as discussed in the next paragraph.

2.1 Limitations and possible improvements of the "Sismabonus" assessment procedure

Several past research works in the literature aimed to evaluate the effectiveness of the Italian "Sismabonus" loss assessment procedure when compared to more refined methodologies (e.g, [24,31]). The results of such investigations highlighted the tendency of the simplified methodology to overestimate (by up to and even over 100% in some cases) the expected economic losses when compared to probabilistic component-based procedures ([31]). These differences are mainly related to the simplified assumptions adopted by the Italian "Sismabonus" procedure. Among others, the use of fixed %RC associated with each LS represents a main simplification. Even if these values have been calibrated by using the extensive database of the repair and reconstruction costs after the L'Aquila earthquake 2009 in Italy ("White Book", [32]), they are provided as aggregated values (with thu very high dispersion) of a large variety building typology, construction materials and occupancy. Thus, the expected loss ratios at different LSs may result significantly different between simplified and refined loss assessment estimation, potentially leading to critical differences when computing the EAL values. Clearly, the use of non-linear static or dynamic response analyses also affects the economic loss estimation.

Yet, looking at the simplified procedure described in [19], a fundamental assumption that may strongly affect the result is represented by the provision to evaluate the earthquake return period related to the PGA capacity value at a specific LS. Instead of performing an ad-hoc probabilistic seismic hazard analysis (PSHA) of the site, the Sismabonus guidelines provide a simplified formulation to compute the return period capacity $T_{r,c}$ (Eq. 1):

$$T_{r,C} = T_{r,D}\ (PGA_C/PGA_D)^{\eta} \tag{1}$$

where $T_{r,C}$ and $T_{r,D}$ are the capacity return period and the demand return period, respectively; PGA_C/PGA_D is the capacity/demand ratio in terms of PGA at a specific LS, while η is a parameter related to the seismic hazard of the size. The guidelines suggest using $\eta = 1/1.41$ as an average value for the whole Italian territory. It is worth mentioning that the PGA values (both capacity and demand) at different LSs are computed considering the code-compliant demand spectra, each one associated with a specific $T_{r,D}$. Thus, it can be noted that using the capacity/demand ratio in terms of PGA or other IM metrics such as the spectral acceleration at the fundamental period $S_a(T_1)$ do not affect the estimation of $T_{r,c}$ (i.e., the same $T_{r,c}$ value would be obtained through Eq. 1).

The formulation reported in Eq. 1 represents a first-order approximation of the hazard curve, or, in other words, a straight line with a fixed angular coefficient (the η value) and passing through to the IM_D-λ_D point for each LS (remembering that $\lambda = 1/T_r$). Clearly, this simplification can strongly affect the results in terms of economic losses, potentially leading to an "unfair" comparison if a more refined definition of the hazard curve is adopted in the advanced loss assessment approaches. For instance, O'Reilly et al. [31] pointed out this problem and decided to adopt the same hazard curve to carry out the comparison between the Sismabonus and the FEMA P-58 loss assessment methodology.

As a possible improvement of the loss-modeling procedure adopted in the Italian guidelines, a second-order approximation for the hazard curve could be adopted. This would result in providing a simple analytical formulation to compute the $T_{r,c}$ (or λ) values for each LS, as in Eq. (1), thus without increasing the computational effort. The general equation of the second-order hazard-fitting solution is reported in Eq. 2:

$$\lambda(IM) = k_0 \exp(-k_2 \ln^2 s - k_1 \ln s) \tag{2}$$

where k_0, k_1, and k_2 are coefficients obtained through a regression analysis. If a second-order biased fitting were adopted (i.e., forcing the second-order polynom to pass through specific points, as suggested by Vamvatsikos [33]), these factors could be easily derived by a simple linear system. Vamvatsikos [33] proved that such a solution can provide a significant improvement in estimating the mean annual frequency of exceedance a specific LS (in line with the SAC-FEMA approach) when compared to a first-order approximation.

As an example, Figure 2 shows the comparison between the first-order approximation provided by the Sismabonus guidelines and a second-order biased fitting for some IM_D-λ_D values provided by the Italian building code, [34]. By comparing the different curves, significant differences can be highlighted in terms of the λ values, especially for lower and higher IM. It is worth mentioning that the lower LS (i.e., O-LS and DC-LS) are expected to have a higher contribution to the EAL value and that the first-order solution tends to overestimate the λ values related to these LSs when compared to the second-order one (as shown in Figure 2). Thus, higher EAL values are expected for the first-order approximation.

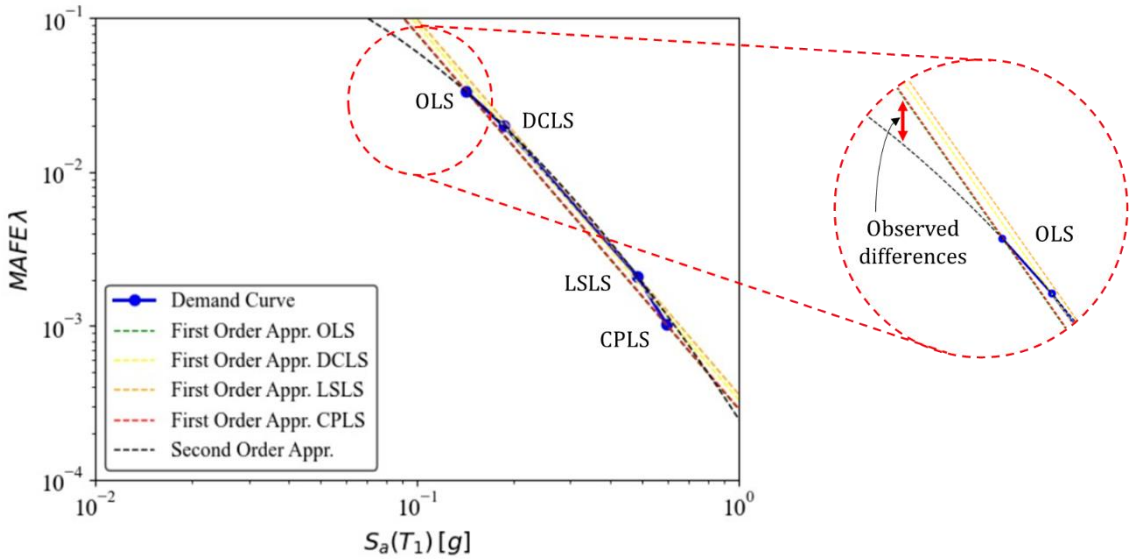

Figure 2: Example of comparison between the first order and the second order approximation of the hazard curve.

The use of a second-order approximation could thus represent a significant improvement in the simplified loss-assessment procedure proposed by the Sismabonus guidelines, also providing a "fairer" comparison with more refined methodologies adopting an enhanced definition of the hazard curve. The effectiveness of this proposed improvement is investigated in the next sections of this research work.

3 CASE-STUDY APPLICATION

3.1 As-Built configuration

The case-study building consists in a three-story Reinforced Concrete (RC) frame located in a high seismicity zone in Center Italy (i.e., L'Aquila). The building is designed for gravity-loads only following an elastic approach based on the concept of "working stresses", and in the absence of the modern "capacity design principles". Fig. 3 shows the geometric features of the building (a), together with the reinforcement details in beams, columns (b) and joints (c). Specifically, stirrups are not provided in the beam-column joints and plain round bars from beams

are hooked-end anchored within the panel. This detail is considered to be the worst configuration for beam-column joints [35]. Considering that the building is poorly detailed and with no capacity design principles, a "weak column-strong beam" system is expected, with brittle local mechanisms potentially leading to global collapse mechanism[1]. The building is thus considered potentially "earthquake- prone", and alternative retrofit strategies have been considered to enhance the seismic performance.

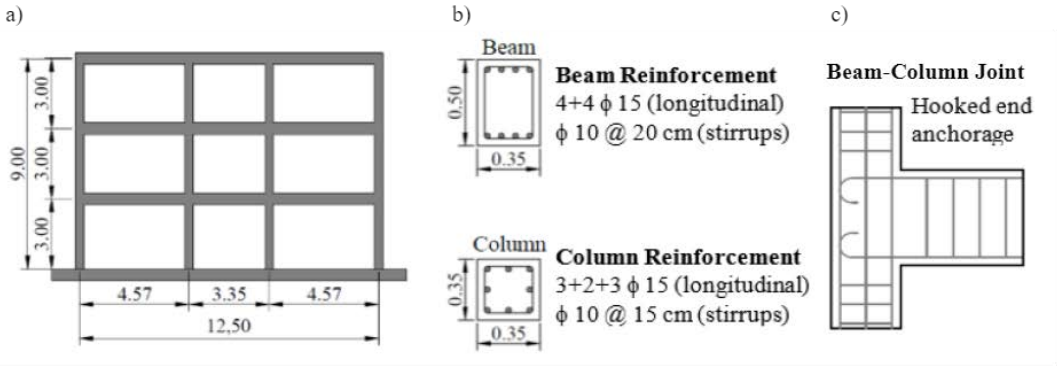

Figure 3: a) Geometric characteristics of the as-built structure, beam and columns cross-sectional area properties and reinforcement, c) beam-column joints reinforcement details.

3.2 Seismic retrofit implementing local strategies

The first two alternatives considered for the seismic upgrading of the as-built structures consist in local interventions using Carbon-Fiber Reinforced Polymers (CFRP) or Concrete Jacketing (CJ). These local interventions aim to modify the "hierarchy of strength" within the beam-column joints subassembly, enabling to attain more desirable flexural (plastic hinge) mechanisms in the beams rather than brittle ones generally expected in the as-built configuration. Furthermore, local interventions can be used to enhance the ductility of structural members through confinement, especially in case of columns subjected to high load conditions.

The first local intervention considered employs CFRP for strengthening beam-column joints [36]. Specifically, such intervention allows to enhance the shear-capacity and confinement of the beam-column joints enabling to delay brittle failure mechanisms and allowing the beam-hinging within the subassemblies, in line with the desirable sequence of events. Furthermore, CFRP can be used for the confinement of members (i.e., especially for columns, both considering partial as well as fully wrapped elements), allowing for an improvement of their ductility and shear capacity [37].

The second local strategy consists in using Concrete Jacketing (CJ). Such technique is widely used as it is characterized by low-costs and does not require specialized labor. Such technique requires to encase the existing member with a newly casted in-place RC jacket. Such technique allows to increase the flexural and shear strength of the member, together with its ductility. Furthermore, if the jacket is continuous in two consecutive floors, it leads to strengthening the beam-column joint panel zone. It is worth noting that the minimum dimension of the jacket depends on the size of the longitudinal and transversal bars adopted, and on the minimum requirements for the concrete cover [38,39].

3.3 Seismic retrofit implementing low-damage external exoskeletons

The latter two alternatives herein used consist of global external exoskeletons implementing low-damage wall and frame systems. The low-damage technology herein considered refers to the PRESSS technology which has been largely tested and extensively investigated for the past

two decades starting from the 1990's at the University of California San Diego (UCSD) and later on at University of Canterbury, Christchurch New Zealand [5, 6, 40], amongst others. Such system, replaces the development of the plastic hinges, expected in monolithic systems, with a controlled rocking & dissipative mechanism at the interface among structural members (e.g., beam-to column, column-to-foundation, wall-to-foundation). The PRESSS technology features two kind of reinforcement. The first one consist of unbonded cables/bars designed to remain elastic and thus enabling the self-centering capabilities of the system at the end of the earthquake shaking by ensuring reduced/negligible residual displacement. The latter consists in internal rebars, or preferably, external and replaceable *"Plug&Play"* dissipaters [40,41], which guarantee the energy dissipation capabilities of the system. Combining the self-centering capabilities together with the energy dissipation ones, a peculiar "Flag-Shaped" hysteresis rule results for the PRESSS technology. One of the key parameters when dealing with the design of PRESSS structures is the "Recentering-Ratio" λ, [42], defined as the ratio between the moment contribution due to post-tension/axial load to the one related to internal rebars or Plug&Play dissipaters. Considering the definition of λ, high values of this parameters are associated with thinner "Flag-Shaped" hysteresis rule, ensuring superior self-centering capabilities of the system. Fig. 4 shows an example of a "jointed-ductile" column-to-foundation connection (a), together with the peculiar hysteresis rule (b).

Furthermore, the PRESSS technology allows to overcome the nowadays well-known problems related to the repairing activities of the structural skeleton (i.e., associated to beams/columns hinging) and the residual/permanent displacements observed in buildings subjected to major earthquakes [43]. In fact, when considering the repairing activities, limited downtime/repair costs are expected in a low-damage re-centering PRESSS-technology system as only the "sacrificial" Plug&Play elements could require replacement after strong earthquakes [44].

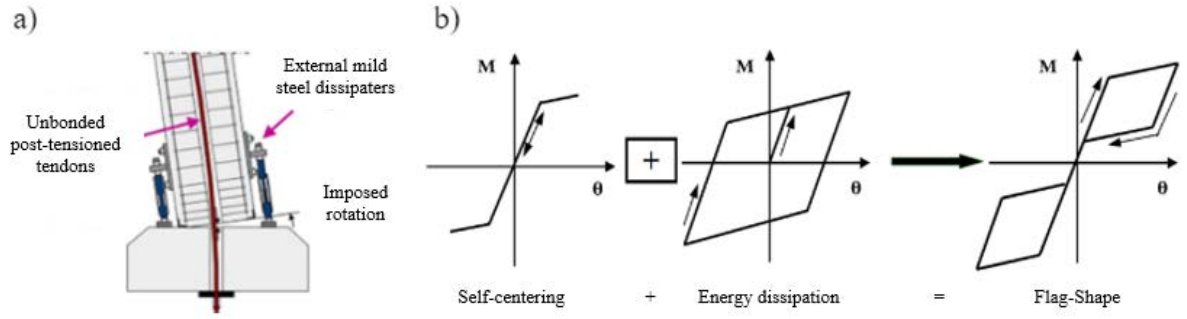

Figure 4: a) Example of a column-to-foundation of a jointed ductile connection with external Plug&Play dissipaters, and b) "Flag-Shaped" hysteresis rule of the PRESSS connections, modified after [42, 44].

3.4 Modelling approach

Seismic response analyses are performed by implementing a two-dimensional (2-D) lumped plasticity model in the structural software Ruaumoko [45]. For the sake of simplicity, fixed base joints (i.e., the soil-structure interaction contribution is neglected), and floor diaphragms are assumed rigid in their plane. Frame members are modelled by mono-dimensional elastic elements with plastic hinges at the end sections (Giberson elements). The plastic hinges' behavior is defined through bi-linear moment-curvature relationships, and the plastic hinge length is evaluated according to [46]. Only for columns, an axial load-moment interaction diagram is also implemented. The shear failure mechanism and the flexural/shear interaction is also evaluated according to the [18]. Rigid links with additional non-linear moment-rotational springs are adopted to model the panel zones, in order to consider the joint capacity and actual

behaviour. More specifically, the non-linear behavior of the rotational springs is characterized by equivalent column moment vs shear deformation relationships, as suggested in [47]. Moreover, in order to account for the influence of the axial load on the joint capacity, an axial load-moment interaction diagram is also implemented. Finally, for all RC structural members, a linear strength degradation is defined, setting a total loss of the moment capacity when a deformation equal to twice the ultimate deformation capacity is achieved (as suggested in [28]).

Concerning the hysteresis behavior of the structural member, the Takeda hysteretic model is implemented for beams and columns. The unloading and reloading stiffness factors are set equal to $\alpha = 0.3$, $\beta = 0.5$ for beams and $\alpha = 0.5$, $\beta = 0.0$ for columns (i.e., a thinner hysteresis loop for columns is considered). Differently, the modified Sina model, [48], is adopted to model the hysteretic behavior of the joint panel. This hysteresis rule allows considering also the "pinching" effect. For non-linear static analyses, a load distribution proportional to the story masses is considered. Yet, for NLTHAs, a tangent stiffness-proportional damping of 5% of the critical one is adopted for all the vibration modes.

Regarding the retrofitted structures, the effects of local interventions (i.e., CFRP or CJ) are modelled by modifying the moment–curvature relationship of the plastic hinges. Clearly, in the case of the Concrete Jacketing intervention, the geometry of the retrofitted columns is also updated in the model. On the other hand, in the case of global interventions (i.e., wall and frame exoskeletons) an additional structural model is implemented and connected to the existing one through pinned rigid links. The structural members of the low-damage exoskeleton are modelled by elastic members with two non-linear rotational springs (working in parallel) at the end section, [49,50]: the first one simulating the re-centering effect of the unbonded post-tensioning cables/tendons and the second one simulating the energy dissipation provided by the external dissipaters. Therefore, a non-linear elastic hysteresis is used for the first rotational spring, while an elastic-plastic rule, based on Ramberg-Osgood hysteresis, is adopted for the second one.

3.5 Record selection and derivation of fragility and vulnerability curves

Fragility analysis allows to define the conditional probability of exceeding different Damage States DSs over a range of Intensity Measures IMs, i.e., $P(DS \geq DS_i|IM)$. In this research work, fragility relationships are derived using the cloud analysis suggested in [51], and then improved considering collapse cases in [52]. The method begins with the selection of a suite of unscaled natural records to perform Non-Linear Time History Analyses (NLTHAs) to evaluate the seismic response of the buildings over a wide range of IM. The records have been selected from the Selected Input Motions for Displacement-based Assessment and Design (SIMBAD) database, [53]. This database comprises 467 three-components records. In this investigation, 150 records are selected, following the approach used in [28]. Specifically, all the 467 ground-motion records are ranked considering the PGA values related to the geometric mean of the two horizontal components. Finally, to select the 150 records to be used, only the horizontal component with the highest PGA is used. No more than 6 records from the same seismic event are selected, as suggested in [54].

By using the results of the 150 NLTHAs it is possible to define a cloud which relates, for each record, an Engineering Demand Parameter (EDP) with an IM. In this case, the Maximum Inter-Story Drift Ratio (MIDR) and the 5%-damped spectral acceleration at the fundamental period, $Sa(T_1)$, are selected as EDP and IM, respectively. In order to perform the fragility estimation, firstly the results of NLTHAs are grouped into collapse (C) and no-collapse (NoC) cases. Specifically, the collapse cases correspond to dynamic instability of the numerical simulations and/or a MIDR larger than a value corresponding to a global strength degradation equal

to 15% (evaluated through a non-linear static analysis), according to [34]. The fragility formulation is defined in Eq. 3:

$$P(DS \geq DS_i|IM) = P(DS \geq DS_i|IM, NoC)\big(1 - P(C|IM)\big) + \\ + P(DS \geq DS\_i|IM, C)P(C|IM) \tag{3}$$

where P(DS≥DSi|IM,NoC) represents the conditioned probability of exceeding a generic DS given an IM and with no collapse occurring; P(C|IM) represents the conditioned probability of having a collapse case given an IM; P(DS ≥ DSi|IM,C) refers to the conditioned probability of exceeding a DS, given an IM and considering that collapse occurs. In this investigation, it is assumed that P(DS ≥ DSi|IM,C)=1, i.e. the DS threshold is always exceeded for the collapse cases.

The EDP vs IM cloud for NoC cases is used to fit a power-law Probabilistic Seismic Demand Model (PSDM), i.e. EDP =aIM^b. The fitted PSDM is thus used to evaluate the P(DS≥DSi|IM,NoC) through a lognormal Cumulative Density Function (CDF). On the other hand, P(C|IM) is defined through a logistic regression, which is deemed suitable to binary variables such as C/NoC cases. Finally, the result obtained through Eq. 3 is converted into a lognormal CDF featured by a median and a logarithmic standard deviation, according to [55].

The vulnerability curves are computed using building-level Damage-to-Loss Ratios (DLRs) for each DS, in order to define a consequence model relating the repair-to-reconstruction cost (i.e., the Loss Ratio, LR) to a given IM. Specifically, in order to compare the results in terms of EAL defined through vulnerability relationship with the prevision related to the method included in the "Italian Guidelines for Seismic Risk Classification of Buildings", [19], the same DLRs used in such guidelines have been selected. The several DSs are defined according to [34] and similarly as in previous work (e.g., [56,57]). Table 1 collects the adopted values of DLRs couples with the DSs.

	DS1	DS2	DS3	DS4	DS5
DLR	7%	15%	50%	85%	100%

Table 1: DLRs considered for the several DSs, defined according to [19].

The LR for a given IM is defined as in Eq. 4.

$$LR(IM) = \sum_{i=1}^{5} \big(F_{DSi-1}(IM) - F_{DSi}(IM)\big) DLRi \tag{4}$$

Where F_{DSi} is the fragility curve for the generic DS, i.e. F_{DSi} = P(DS≥DSi|IM). It is worth nothing that such approach allows the assessment of the earthquake-induced losses using the DLRs defined at a building level. Even though more refined loss assessment procedure (i.e., component-based) are available [21], the building-level approach is herein deemed appropriate to only identify the best retrofit strategy, as already discussed in the previous section 2. Finally, by combining the vulnerability curves with the site-specific hazard analysis, it is possible to define the EAL, according to Eq. 5.

$$EAL = \int_0^{\infty} LR(IM) \left|\frac{d\lambda_{IM}}{dIM}\right| dIM \tag{5}$$

where λ_{IM} is the Mean Annual Frequency of Exceedance (MAFE), defined from the hazard curve, for the generic IM.

4 RESULTS AND DISCUSSIONS

4.1 Performance assessment in the as-built configuration

In order to assess the seismic performance of the case-study structure in the as built configuration, a non-linear static (pushover) analysis has been carried out following the approach described in section 3.4. The results of the analysis highlight that the failure mechanism of the structure is mainly governed by the brittle failure of exterior and interior beam-column joints, as expected for a pre-code building. Fig. 5a shows the pushover curve with the identification of the DSs and the plastic mechanisms expected for DS3. Specifically, as suggested in [57], DS1 is identified when a displacement equal to $0.7d_y$ is achieved, where d_y represents the equivalent yielding displacement of the structure, which correspond to the attainment of DS2. Such value is identified by a bilinearization of the pushover curve, following the instruction of [34]. In particular, the pushover curve is bi-linearized using as an ultimate point the one relative to the attainment of the Life-Safety Limit State (LS-LS), which correspond to DS3. The bilinear curve is plotted in Fig. 5a (dashed line). DS3 and DS4 are identified by the first element which reach $3/4\theta_U$ and θ_U, where θ_U stands for the ultimate rotation. Finally, DS5 is attained when a global strength reduction equal to 15% is observed. After that, the response of the Multi-Degree-of-Freedom (MDoF) system is converted into an equivalent Single-Degree-of-Freedom (SDoF) within an Acceleration-Displacement Response Spectrum (ADRS) domain. In order to define the performance points, the Capacity Spectrum Method (CSM, [29]) is adopted. Such method, corresponding to "Method B" in the Italian Design Code NTC2008 [34], is preferred to the N2 method [30], (i.e., "Method A" in the NTC2018), as a previous work by the authors [58] demonstrated that CSM seems to be more conservative in evaluating the seismic risk class of a building.

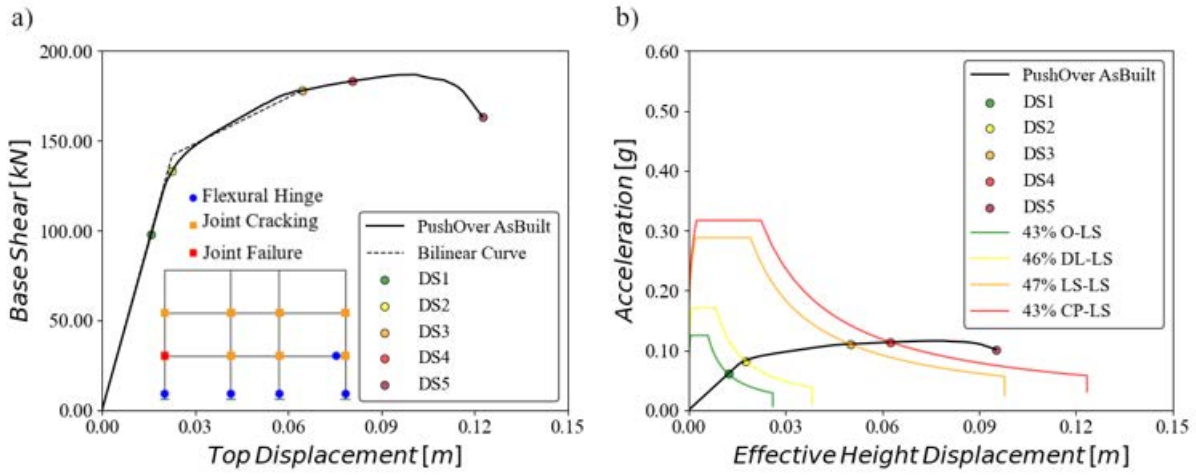

Figure 5: a) PushOver curve of the as-built configuration and b) identification of performance points within the ADRS domain.

The performance points are evaluated considering four intensity level earthquakes. Specifically, the Operational Limit State earthquake (O-LS), the Damage-Control Limit State (DC-LS) earthquake, the Life-Safety Limit State (LS-LS) earthquake and the Collapse-Prevention Limit State (CP-LS) earthquake. In order to define the performance points, the elastic spectra of O-LS and DC-LS have been scaled until the attainment of the corresponding DSi (i.e., DS1 and DS2). For the ultimate limit state earthquakes (i.e., LS-LS and CP-LS), the damped spectra have been used and scaled until DS3 and DS4. Specifically, the equivalent viscous damping

has been defined following the "Method B" of the Italian Building Code [34] using a factor *k* equal to 0.33, which is suggested by the code for structure with low-dissipation capabilities, as expected for pre-code buildings. Fig. 5b shows the definition of the performance points within the ADRS domain.

Finally, the fundamental period (T_1) and the MIDR thresholds for the DSs in the as-built configuration are listed in Table 2.

	DS1	DS2	DS3	DS4	DS5	T_1
As-Built	0.21%	0.30%	0.92%	1.11%	1.75%	0.87 sec

Table 2: MIDR for the DSs and fundamental period of the as-built configuration

4.2 Fragility estimation

Using the results from the previous paragraph, the safety evaluation and loss assessment is carried out. Specifically, the results have been obtained considering both a practical, pushover-based approach, as well as a more refined one based on NLTHAs. Specifically, NLTHAs have been performed with the aforementioned 150 natural records. The results of such analysis have been used to define a PSDM of the as-built configuration.

Fig. 6a shows the spectra of the selected records, plotted together with the mean and the code spectra for the site of interest (i.e., L'Aquila). Nevertheless, it is worth remembering that the cloud analysis (herein adopted) does not require a site-specific hazard-consistent record selection. Fig. 6b shows the PSDM, which is defined as $EDP = aIM^b$, with a = 2.306 and b = 0.789.

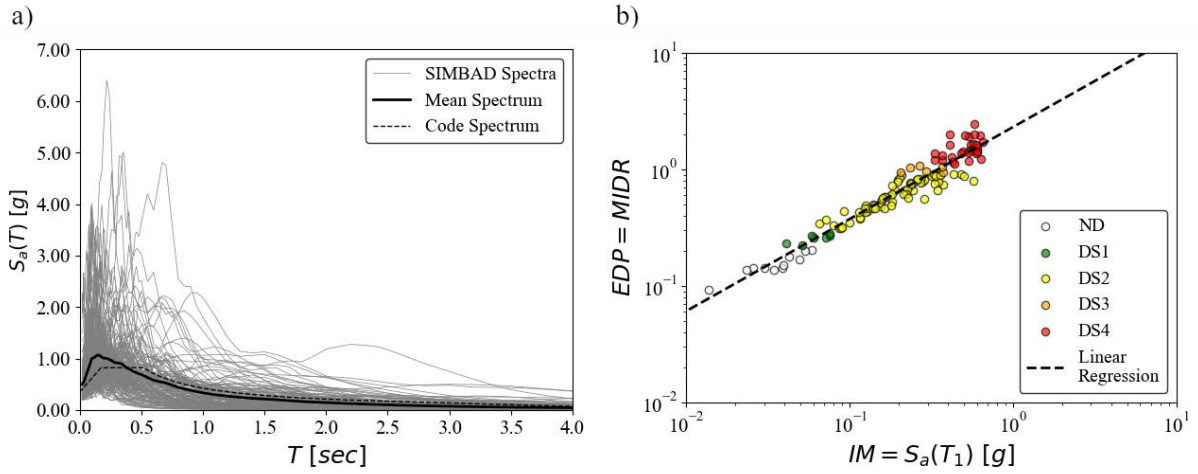

Figure 6: a) 150 records selected from the SIMBAD database together with the mean and code spectra, b) PSDM for the as built configuration.

Fragility estimation is thus performed by using the fitted power-law PSDM and the logistic regression built considering the collapsed and non-collapsed cases (Fig. 7a), as explained in Section 3.5.

Furthermore, in order to investigate the effectiveness of an alternative simplified approach, fragility relationships are also derived using the results of the non-linear static analysis. In this case, the median value of the fragility curve for each DS is defined as the spectral acceleration (Sa(T)) of the scaled spectra previously defined, following the CSM. In order to define the fragility for DS5, the CP-LS earthquake has been scaled, using the same approach outlined previously for the other DSi, until the ultimate point of the pushover curves. Yet, default

dispersion values are selected, i.e. $\beta = 0.450$, according to [26]. Fig. 7b compares the fragility functions for all the DSs derived using both a pushover-based approach (PO) and a more refined Non Linear Time History Analysis, NLTHA (TH). The median values of the fragilities, μ, and the logarithmic standard deviations, β, are summarized in Table 3 for both the approaches.

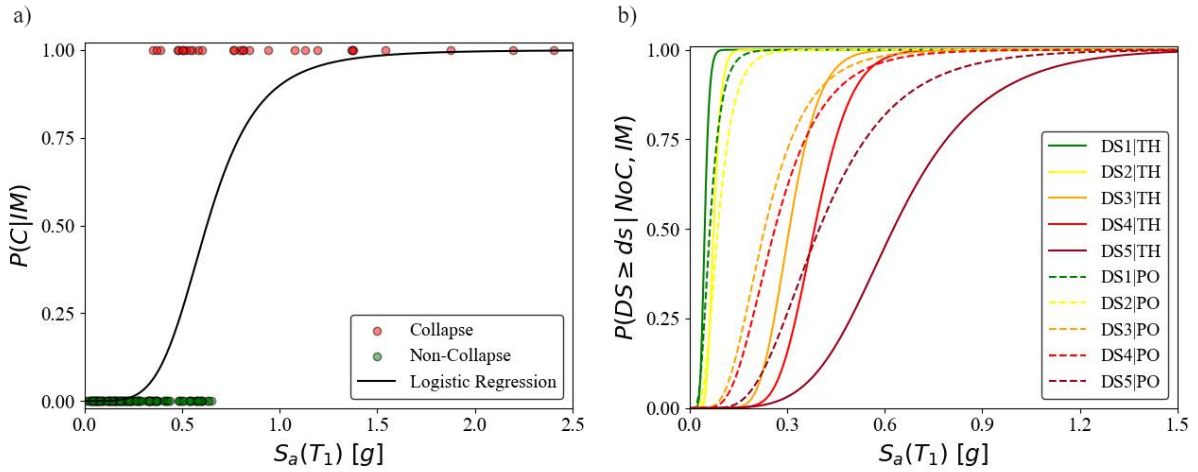

Figure 7: a) Logistic regression, and b) fragility curves derived both using the pushover-based approach as well as the one based on NLTHAs and cloud methodology accounting for collapse cases.

	$\mu_{DS,PO}$ [g]	$\beta_{DS,PO}$	$\mu_{DS,TH}$ [g]	$\beta_{DS,TH}$
DS1	0.063	0.450	0.047	0.242
DS2	0.087	0.450	0.074	0.242
DS3	0.231	0.450	0.306	0.238
DS4	0.264	0.450	0.384	0.235
DS5	0.399	0.450	0.626	0.350

Table 3: Median and logarithmic standard deviation values for the fragility curves in the as built configuration.

Results highlight a relatively good agreement between the median values of the fragility relationships obtained though the pushover-based and the more refined NLTHA-based procedures. However, significant higher dispersion values are observed for the simplified methodology (PO) when compared to the more refined one (TH), for all the considered DSs. It is also interesting to note that, on one hand, as expected, PO methodology tends to underestimate the seismic performance of the structure at the higher DSs (i.e., DS3-DS5), thus returning a higher fragility of the structure (i.e., lower μ values) than the TH method. On the other hand, this trend seems to be inverted for the lower DSs (i.e. DS1, DS2), where higher μ values are obtained for the PO method if compared to the TH one. This result is expected to affect the evaluation of seismic performance of the structure in terms of economic losses, as discussed in the next section.

4.3 Safety evaluation and loss assessment in the as-built configuration

The safety evaluation of the building consists in defining the "Safety-Index", IS-V. According to [19], such value is defined as the ratio between the capacity of the structure to the demand on an equivalent newly designed building at the LS-LS. The IS-V is calculated considering either the pushover-based approach (i.e., through the CSM) and using the results of the probabilistic-based approach. Specifically, in the latter case, the IS-V is evaluated considering as seismic capacity of the structure the median value of the fragility curve at DS3. The as-built

structure scores 47% and 63% IS-V considering the pushover-based approach or the NLTHAs one, respectively. This result confirms that the non-linear static approach seems to be conservative with respect to the non-linear dynamic one, as can be noticed even from the comparison for fragility curves related to DSi associated to the ultimate limit states.

The loss assessment is carried out by evaluating the EAL considering four alternative approaches: i) the procedure described in [19], referred to as the PAM value (according to the nomenclature of [19]); ii) a refined version of the procedure described in [19] (PAM_{Ref}), considering a second-order biased fit of the hazard curve, as previously discussed in section 2.1; iii) using Eq. 5 and considering the vulnerability model derived through the simplified pushover-based approach (EAL_{Frag_PO}); and iv) the same methodology as iii), but considering the vulnerability model derived through more refined NLTHAs (EAL_{Frag_TH}). When the approaches from ii) to iv) are used, the coefficients of Eq.2 must be calculated. Specifically, in this case, a wide interval has been considered for the second-order biased fit proposed in [33]. In order to define an analytical formulation for the hazard curve, three IM-λ_{IM} couples must be selected to define the three coefficients of Eq.2. As the main contribution to EAL is related to the higher values of λ_{IM} (i.e., lower LSs), the IM-λ_{IM} couples related to O-LS, DC-LS and LS-LS earthquakes are herein considered. The resulting coefficients are: k_0=0.000248, k_1=3.213 and, k_2=0.359.

Fig. 8a shows the vulnerability curves (both derived from PO and TH approach), while Fig. 8b shows the PAM and EAL curves derived following the four approaches defined before.

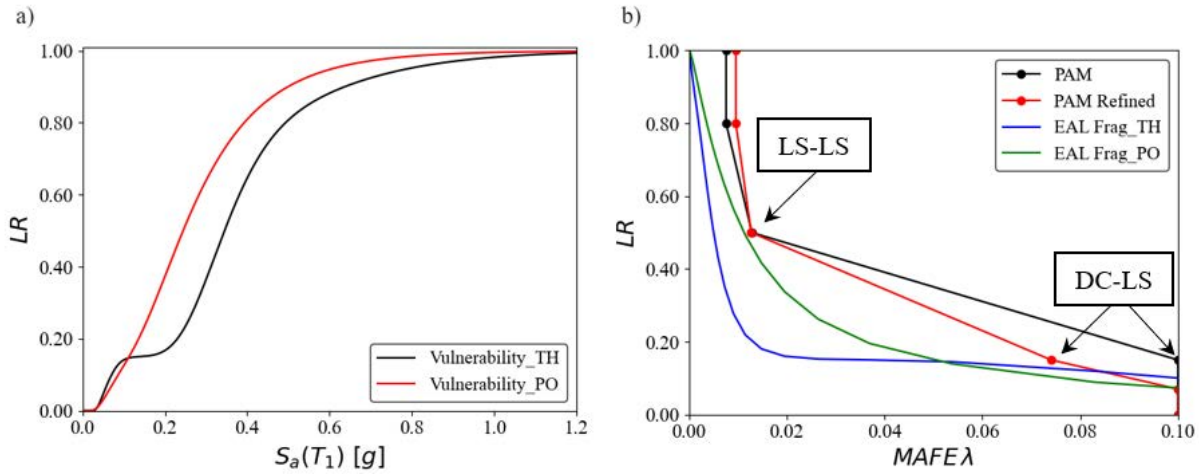

Figure 8: a) Vulnerability curves and b) EAL and PAM curves for the as-built configuration. LR: Loss Ratio

Table 4 reports the PAM and the EAL values defined through the four approaches, together with the IS-V values defined considering the pushover and time-history approaches.

The results of the loss assessment show a reduction of the expected losses if the refined PAM is used with respect to the traditional method. This was expected as the use of the second-order biased fitting allows to use much more reliable values of the λ_{IM} in the definition of the curve. In fact, the major differences among the refined and the traditional method are observed for the DC-LS, which attainment is expected for frequent earthquakes, where the correction introduced by the second-order biased fitting is crucial.

When dealing with the PAM method, it should be considered that the curve is built connecting only few points (λ_{IM}, *LR*) depending on the performance of the building and on the Loss-Ratio related to the achievement of a specific LS. On the other hand, if a probabilistic-based approach is used (either PO or TH), the derived curve is continuum. In other words, this

approach allows for an estimation of the LR for each λ_{IM}, while in the PAM methodology only few LR- λ_{IM} points can be estimated. For this reason, it is quite easy to understand why the probabilistic approach based on pushover analysis estimates lower value of EAL with respect to the refined PAM method, even considering the closeness of the curves in correspondence of the PAM's points representing the attainment of DC-LS and LS-LS. Therefore, in order to improve the simplified PAM tool, further LRs could be defined for intermediate structural performances among the DC-LS and the LS-LS.

Considering the EAL curve obtained through NLTHAs, it can be noted that for higher values of λ_{IM}, the time-history approach overestimates the losses with respect to the pushover-based approach. This is justified by the fact that for low IM, the vulnerability curve derived through time-histories is higher with respect to the one derived through pushover (Fig. 8a), as a result of the lower median values of fragilities estimated through NLTHAs with respect to PO approach for both DS1 and DS2. This trend is inverted for higher IM, justifying the crossing among the EAL curves (Fig. 8b). Furthermore, the EAL derived through time-history is lower with respect to the one defined through pushover since for higher IM, the difference among the vulnerability curves is much higher with respect to the first branches of the curves.

Finally, the seismic risk class of the as-built structure has been defined according to [19]. Such class is defined as the minimum class among the one related to the Safety-Index and the Expected Annual Losses (i.e., PAM or EAL). In this case, four classes have been defined according to the previous analyses. In the first three cases, the pushover-based method has been used, and the differences are related to the method used to assess the EAL; in the latter, results based on NLTHAs have been used. Table. 4 collects the classes related to the Safety Index and the Expected Annual Losses, as well as the final seismic risk classes for all the considered methodologies.

Case	IS-V	$Class_{IS\text{-}V}$	PAM/EAL	$Class_{PAM}$	Seismic Risk Class
PO-PAM	47%	C	3.93%	E	E
$PO\text{-}PAM_{Ref}$	47%	C	3.44%	D	D
PO-EAL	47%	C	2.34%	C	C
TH	63%	B	1.82%	C	C

Table 4: Definition IS-V and PAM/EAL values together with the seismic risk class of the as-built configuration following the alternative approaches.

In all cases, the PAM/EAL governs the definition of the seismic risk class, but as expected, for the same building, different classes have been obtained according to the different estimation of the losses.

Even though the approach based on NLTHAs is considered as the more reliable, in the following (i.e., for the alternative retrofit strategies) only the approaches from i) to iii) have been considered in this preliminary work for the loss assessment, and only the pushover-based approach has been considered for the definition of the Safety-Index, IS-V. This is justified by the fact that for both the Safety-Index, as well as for the loss assessment, the pushover-based method is conservative. Furthermore, the obtained seismic risk class, at least in the as-built configuration, is the same using the probabilistic pushover-based method and the one based on NLTHAs. In addition, the focus on pushover-based approach is also related to the fact that such analyses are deemed as the best compromise between accuracy and simplicity, even considering the suitability for practitioners, when compared to more accurate, but even more complex and time consuming NLTHAs.

4.4 Performance assessment of the retrofitted configurations

As in the case of the as-built structure, the performance assessment of the retrofitted alternatives has been carried out. As stated before, the retrofit alternatives consist of two local strategies (i.e., use of CFRP and CJ), and two global interventions consisting in the implementation of external exoskeletons using external walls (Exo-Wall) and frames (Exo-Frames), respectively.

In the first case (i.e., use of CFRP), the external and internal beam-column joints at the first two stories have been strengthened following the procedure available in [36]. Furthermore, the base columns have been fully wrapped through CFRP in order to improve their ductility. The procedure used to consider the effect of the confinement through CFRP is available in [37].

Following a similar approach, the second retrofit alternative consists in using CJ to enhance beam-column joints strength and both strength and ductility of columns. In this case the CJ have been implemented along the entire height of the building for external columns and only at the ground floor for the internal ones. In the latter case, even the internal beam-column joints of the first story result strengthened. Fig. 9a shows the pushover curves of the retrofitted buildings using local intervention compared with the one of the as-built structure. Fig. 9b shows a schematic illustration of the two local interventions implemented. The results clearly show how the modification of the "hierarchy of strength" allows to improve the maximum allowable displacement in both retrofitted structures as a result of the achievement of a more desirable inelastic mechanism.

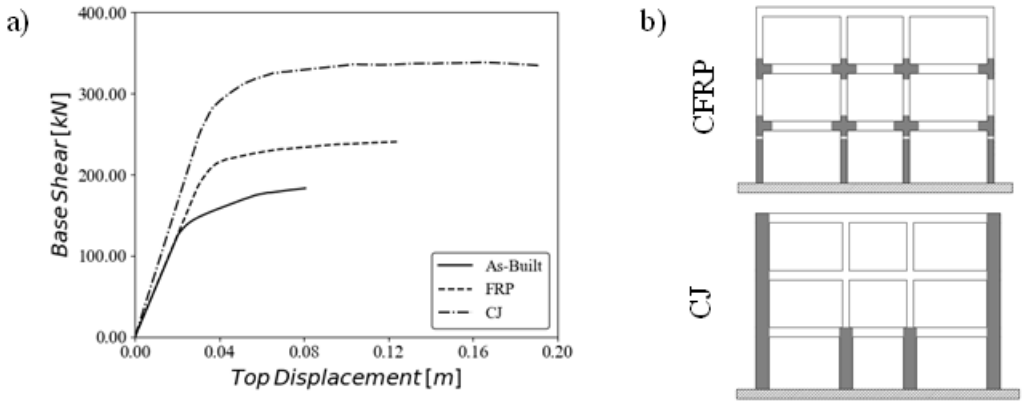

Figure 9: a) Pushover curves of the local retrofit alternatives compared with the one of the as-built configuration, and b) schematic representation of the local alternatives implemented

Furthermore, it is possible to note a slight increase of strength in the CFRP configuration, whilst in case of CJ it is possible to note a considerable improvement of the strength, together with an increase of the stiffness.

Considering the global intervention, exoskeletons consisting both in wall as well as frame systems have been implemented considering the low-damage PRESSS technology. Both the retrofit options have been designed following the Displacement-Based Retrofit (DBR) procedure available in [44,59] for wall and frame systems, respectively. The main objective of such procedure is to prevent the existing building from reaching and exceeding its failure displacement profile. For this reason, the maximum allowable displacement derived through the seismic assessment of the as-built configuration is herein used to design the exoskeletons. In particular, in order to be consistent with the Italian Building Code [34], the maximum allowable

displacement has been set as the one for which the as-built configuration attains DS3 (i.e., the LS-LS). The recentering-ratio herein used is λ=1.75.

Fig. 10a compares the pushover curves of the retrofitted structures with the one of the as built configuration. It is possible to note that the implementation of the exoskeletons increase both the strength as well as the stiffness of the system. Furthermore, it is possible to note an increase in the maximum allowable displacement. This is a result of the added stiffness which forces the as-built structure to deform in a more regular manner, redistributing the inelasticity along the height (i.e., avoiding to concentrate it in reduced zones). Finally, to prove the potentiality of the PRESSS technology in terms of reduction of the residual displacement, a cyclic non-linear static (push-pull) analysis has been carried out for the retrofitted configuration consisting in the frame exoskeleton, Fig. 10b.

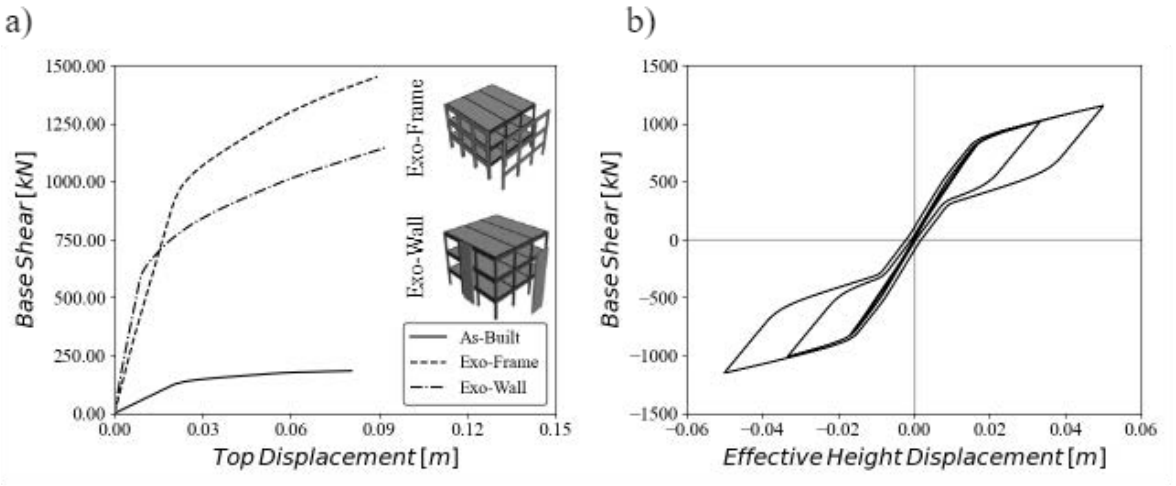

Figure 10: Pushover curves of the global retrofit alternatives compared with the one of the as-built configuration, and b) cyclic bob-linear static (push-pull) analysis in case of frame-type exoskeleton.

4.5 Safety evaluation and loss assessment for the alternative retrofit strategies

Using the results from non-linear static (pushover) analyses from section 4.3, and adopting the same methodology outlined in section 4.2 for the as-built configuration, the safety evaluation and loss assessment for each retrofit strategy have been performed. Firstly, the Safety-Index IS-V has been evaluated for the retrofit alternatives and the obtained values are listed in Table. 5.

Case	IS-V	Class (IS-V)
As-built	47%	C
CFRP	73%	B
CJ	113%	A^+
Exo-Wall	132%	A^+
Exo-Frame	141%	A^+

Table 5: IS-V value and Risk Class$_{_IS\text{-}V}$ for each retrofit configuration.

From the IS-V values, it is possible to note that in the case of exoskeletons, even targeting 100% IS-V in the DBR procedure, higher values are obtained. This is mainly related to the overstrength introduced in the design process with respect to the base shear to be carried out by the exoskeleton considering the results of DBR procedure. Furthermore, when the exoskeleton

is implemented, the added stiffness tends to improve (i.e., regularize) the inelastic deformation mechanism of the existing structure and, as a result, the achievement of DS3 moves towards higher values of maximum allowable displacement for the retrofitted structure. Yet, the as-built deformation threshold at DS3 has been used as a design displacement for the design of retrofitted configuration.

After that, the loss assessment has been carried out. Fig. 11 shows the comparison of the PAM/EAL curves defined through the pushover-based approach for all the retrofit alternatives, i.e. a) CFRP, b) CJ, c) Exo-Wall, and d) Exo-Frame.

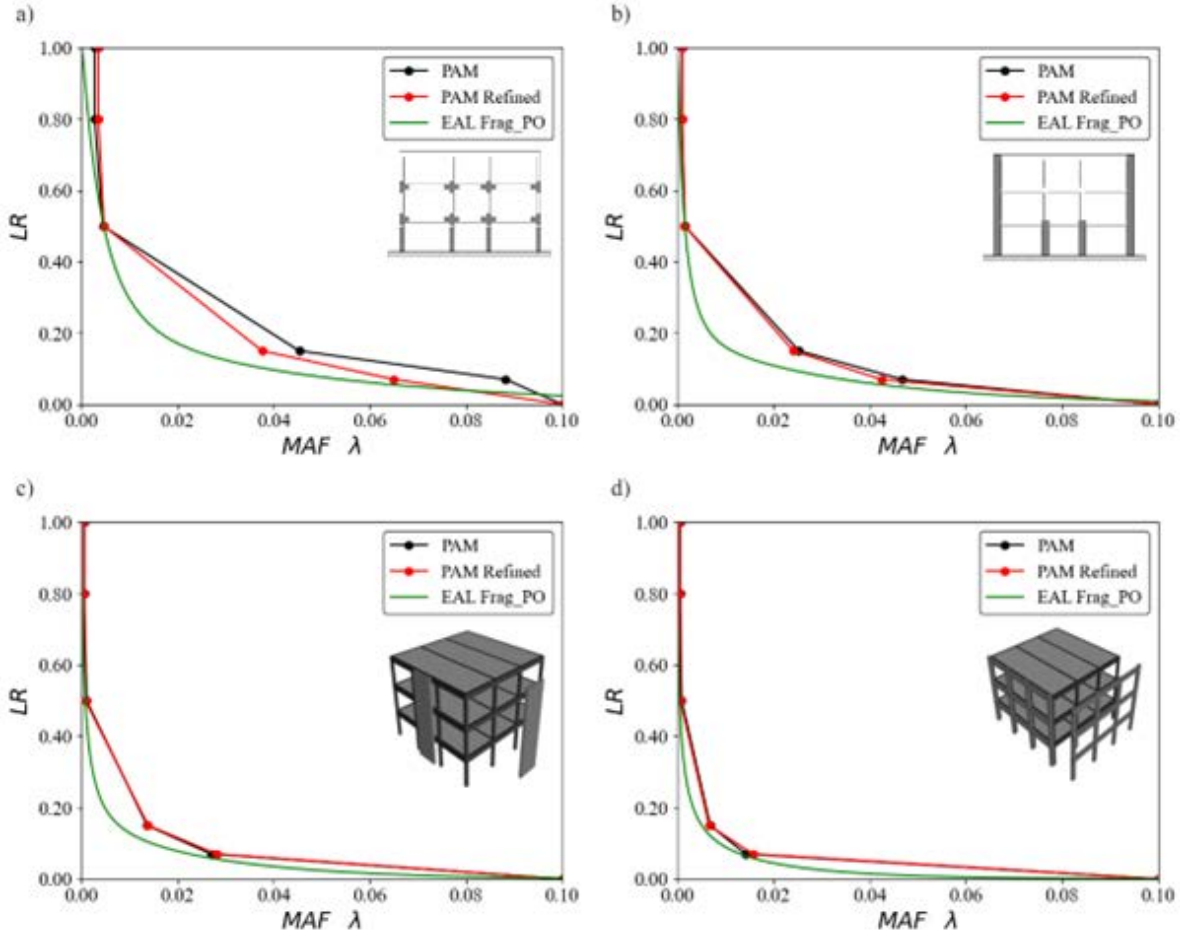

Figure 11: Comparison among PAM/EAL curves for the alternative retrofit strategies: a) CFRP, b) CJ, c) Exo-skeleton-Wall, and d) Exosckeleton-Frame

From the figure, it is possible to note that the proposed improvement of the PAM is important especially when dealing with poor-performing structures, e.g., existing structures in their as-built configuration, or retrofitted structures where the retrofit strategies/techniques do not allow to achieve a similar performance of new buildings, as in the case of CFRP herein presented (Fig. 11a). This result was expected since the proposed refined PAM methodology provides a significant improvement in estimating the performance of the structure at lower LSs in terms of λ_{IM}, as also highlighted by Fig. 2. However, even considering the worst seismic performance obtained with retrofitted structures (i.e., CFRP in this exercise), at least the same PAM class is obtained, differently from the as-built configuration. Instead, considering structures that perform well (e.g., new buildings or retrofitted structures whose seismic performance is similar to new buildings), even if a first-order approximation of the hazard curve is implicitly considered

as in the approach proposed by the [19], the error in defining λ_{IM} is limited. This is mainly related to the obtained capacity values in terms of IM (e.g., PGA, Sa(T1)), which are proximal to the demand ones for newly-designed structures, thus the method typically does not require a large extrapolation of the λ value from the fitted hazard curve. Considering the comparison with the EAL curve derived from vulnerability curves (green line in Fig. 11), the same considerations previously outlined are still valid and lower LR values are obtained for each λ_{IM} with respect to the PAM (both classical and refined) methodology.

Furthermore, Table 6 collects the EAL values and the associated classes evaluated through the alternative methodologies (i.e., PAM, PAM_{Ref}, and the probabilistic approach referred to as EAL in the table) for each considered retrofit technique.

Retrofit Solution	PAM	$Class_{PAM}$	PAM_{Ref}	$Class_{PAMRef}$	EAL	$Class_{EAL}$
CFRP	2.23%	C	1.92%	C	1.33%	B
CJ	1.33%	B	1.27%	B	0.78%	A
Exo-Wall	0.90%	A	0.90%	A	0.54%	A
Exo-Frame	0.65%	A	0.64%	A	0.35%	A^+

Table 6: PAM and EAL values and Risk Classes for the retrofit alternatives.

The seismic risk class has been defined for each retrofit alternative, considering all the approaches used to define the EAL, according to the [19]. Table 7 reports the results of the seismic risk classification compared with the as-built configuration.

Case	$Risk_{PAM}$	$Risk_{PAMRef}$	$Risk_{EAL}$
As-Built	E	D	C
CFRP	C	C	B
CJ	B	B	A
Exo-Wall	A	A	A
Exo-Frame	A	A	A^+

Table 7: Seismic risk class for the retrofit alternatives.

In particular, it is possible to note that for all the retrofit alternatives both the traditional as well as the refined PAM return the same seismic risk class, pointing out once again the importance of the refinement method especially for poor-performing structures. In fact, it is worth noting that the traditional PAM method would suggest that the implementation of the CFRP retrofit solution is able to provide an enhancement of two seismic-risk classes with respect to the as-built structure; however, the proposed refined PAM method and the probabilistic approach return an enhancement of only one class for this retrofit technique. In general, in this specific study, if the class is defined based on the probabilistic-based EAL approach, a superior seismic-risk class by one level is obtained for all the alternative retrofit solutions, except for the exoskeleton wall solution.

Results of the performed investigation highlight the efficiency of the exoskeleton systems both considering the Safety Index as well as the Expected Annual Losses when compared to local strategies, especially to the CFRP configuration. Furthermore, as pointed out in [60], the actual EAL of solutions implementing low-damage exoskeletons should be even lower. In fact, the DLRs used in this case do not take into account the superior performances of the PRESSS technology if compared to traditional monolithic systems. In the low-damage technologies, the development of the plastic hinge is replaced with a controlled rocking mechanism, which allows

to drastically reduce both costs and time of repairing. For this reason, the ongoing research activities are focusing on the use of refined component-based loss-assessment methodologies [21], as already done in [25] to prove the improved performance of newly-designed integrated low-damage buildings, if compared to new buildings designed using traditional solutions.

5 CONCLUSIONS

In this research work, the effectiveness, and thus further justified attractiveness, of seismic retrofit solutions based on low-damage exoskeletons has been investigated and discussed. More specifically, the considered solution consists of additional high-seismic-performance structural systems (either in the form of moment-resistant frames or shear walls) entirely implemented from the outside of the building and characterized by a peculiar, controlled rocking & dissipative mechanism according to the PREcast Seismic Structural Systems (PRESSS) technology.

The benefits derived from the implementation of exoskeleton systems (in terms of both safety and economic losses) have been investigated through an illustrative application to a case-study existing building, designed for gravity-loads-only. Firstly, the seismic performance of the as-built structure has been assessed through either non-linear static or non-linear dynamic time history analyses (NLTHAs). Both analysis methods have been used to evaluate the "Safety-Index" (IS-V, according to the Italian "SismaBonus" guidelines [19]) and the Expected Annual Losses (EAL). Specifically, the latter has been computed using different alternative methodologies, involving: (i) the simplified approach proposed in [19]; a refined version of the latter, herein proposed, considering a second-order biased fitting of the hazard curve; and (iii) a building-level probabilistic-based approach using either the results of the pushover analysis or the NLTHAs.

Results highlighted that the as-built structure shows poor seismic performance, mainly due to the absence of "capacity design" principles. Moreover, the use of the proposed refined version of the "SismaBonus" approach [19], allowed for a better (and "fairer") comparison of the results in terms of EAL between the simplified and the more refined probabilistic-based approaches. It has been observed that such an improved simplified procedure returned significantly lower values of EAL than the classical approach and provided a more accurate estimation of such quantity (considering the probabilistic approaches as benchmark values).

Moreover, alternative retrofit strategies/techniques have been considered in the investigation, in order to perform a comparison between the Exoskeleton (frame or wall) systems and more traditional solutions (i.e., concrete jacketing, CJ, and fiber-reinforced polymer, FRP). Safety evaluation and loss assessment have been carried out for each considered alternative retrofit solution. Results pointed out that the implemented local retrofit intervention consisting in the CFRP only allow for a limited improvement in terms of safety while the exoskeleton solutions (both in the form of frames and walls) and CJ provide IS-V values even higher than 100% (i.e., capacity/demand ratio at the Life-Safety Limit State higher than 1). Furthermore, a significant reduction in terms of EAL values has been observed for exoskeleton solutions when compared to the traditional local strengthening ones. In fact, the implementation of global strategies leads to enhanced seismic risk classes if compared to local strategies.

The results presented in this research work confirm the high potential of low-damage exoskeleton solutions for the seismic retrofitting of existing structures. Even if the results already highlight significant improvements of the seismic performance of the existing structure when this retrofit solution is implemented when compared to more traditional retrofit solutions, additional potential advantages can be investigated as future developments both in terms of methodology as well as technology. For instance, instead of using a fixed building-level damage-to-loss model, a more refined loss assessment investigation can be performed following a fully-probabilistic component-based approach, (e.g., the approach reported in [21]), in order to

emphasize the benefits related to the low-damage solutions. Moreover, following the recent objectives in terms of sustainability at the international level, the use of low-damage solutions based on eco-friendly materials like timber (e.g., Pres-Lam technology) can be investigated within a Life-Cycle Analysis (LCA) approach.

REFERENCES

[1] S. Pampanin, Controversial aspects in seismic assessment and retrofit of structures in modern times: Understanding and implementing lessons from ancient heritage. *Bull. New Zeal. Soc. Earthq. Eng.,* **39**,120–134, 2006.

[2] A. Marini, C. Passoni, A. Belleri, F. Feroldi, M. Preti, G. Metelli, P. Riva, E. Giuriani, G. Plizzari, Combining seismic retrofit with energy refurbishment for the sustainable renovation of RC buildings: a proof of concept. *Eur. J. Environ. Civ. Eng.,* **8189**, 1–21, 2017.

[3] D. Di Vece, S. Pampanin, Combined retrofit solutions for seismic resilience and energy efficiency of reinforced concrete residential buildings with infill walls. *18th ANIDIS conference,* Ascoli Piceno, Italy, September 15-19, 2019.

[4] M.J.N. Priestley, Overview of PRESSS research program. PCI Journal, 36(4), 50–57, 1991.

[5] J. Stanton, W.C. Stone, G.S. Cheok, A Hybrid Reinforcement Precast Frame for Seismic Regions. PCI Journal, 42(2), 20-32, 1997.

[6] M.J.N. Priestley, S. Sritharan, J.R. Conley, S. Pampanin, Preliminary results and conclusions from the PRESSS five-story precast concrete test building. PCI Journal, 44(6), 42–67, 1999.

[7] S. Pampanin, Reality-check and renewed challenges in earthquake engineering: Implementing low-damage systems - From theory to practice. Bull. NZ . Soc. Earthq. Eng., 45, 137–160, 2012.

[8] S. Pampanin. Towards the "ultimate earthquake-proof" building: Development of an integrated low-damage system. *Perspectives on European Earthquake Engineering and Seismology,* **2,** 321-358, 2015.

[9] Pampanin, S., NextGen Building Systems - S4: Seismically Safer, Sustainable and Smart - Raising the Bar to Enhance Community Resilience and Sustainability. *In: Vacareanu, R., Ionescu, C. (eds) Progresses in European Earthquake Engineering and Seismology. ECEES. Springer Proceedings in Earth and Environmental Sciences*. Bucharest, Romania, September 4-9, 2022.

[10] S. Pampanin, J. Ciurlanti, S. Bianchi, M. Palmieri, D. Grant, G. Granello, A. Palermo, A. Correia. Overview of SERA project: 3D shaking table tests on an integrated low-damage building system. *4th international workshop on the seismic performance of non-structural elements (SPONSE)*, Pavia, Italy, May 23-23, 2019.

[11] S. Pampanin, J. Ciurlanti, S. Bianchi, D. Perrone, M. Palmieri, D.N. Grant, G. Granello, A. Palermo, A. Filiatrault, A. Campos Costa, P.X. Candeias, A.A. Correia, Enhancing seismic safety and reducing seismic losses: overview and preliminary results of SERA project – 3D shaking table tests on an integrated low-damage building system. *17th World*

Conference on Earthquake Engineering (17WCEE), Sendai, Japan, September 13-18, 2020.

[12] S. Bianchi, J. Ciurlanti, D. Perrone, A. Filiatrault, A.C. Costa, P.X. Candeias, A.A. Correia, S. Pampanin, Shake-table tests of innovative drift sensitive nonstructural elements in a low-damage structural system. *Earthq. Eng. Struct. Dyn.*, 2021.

[13] A.S. Tasligedik, S. Pampanin, Rocking Cantilever Clay Brick Infill Wall Panels: A Novel Low Damage Infill Wall System, J. Earthq. Eng. **21**, 2017.

[14] P. Morandi, R.R. Milanesi, G. Magenes, Innovative solution for seismic-resistant masonry infills with sliding joints: in-plane experimental performance. *Eng. Struct.* **176**, 719–733, 2018.

[15] A.S. Tasligedik, S. Pampanin, A. Palermo, Low damage seismic solutions for non-structural drywall partitions. *Bull. Earthq. Eng.* **13**, 1029–1050, 2015.

[16] A. Baird, A. Palermo, S. Pampanin. Controlling seismic response using passive energy dissipating cladding connections. *2013 New Zealand Society for earthquake engineering (NZSEE) conference*, Wellington, NZ, April 26-28, 2013.

[17] S. D'Amore, S. Bianchi, J. Ciurlanti, S. Pampanin, Seismic assessment and finite element modeling of traditional vs innovative point fixed glass facade systems (PFGFS). *Bulletin of Earthquake Engineering*, 1-33, 2023.

[18] New Zealand Society for Earthquake Engineering. *The seismic assessment of existing buildings - technical guidelines for engineering assessments*. Wellington, New Zealand, 2017.

[19] Italian Ministry of Infrastructures and Trasport. *Linee guida per la classificazione del rischio sismico delle costruzioni*. (in Italian). Ministry Decree n.65, Allegato A, Rome, Italy, 2017.

[20] C.A. Cornell, H. Krawinkler, *Progress and challenges in seismic performance assessment*. PEER Cent News, 2000.

[21] Federal Emergency Management Agency. *Seismic Performance Assessment of Buildings, Volume 1 – Methodology. Federal Emergency Management Agency*. Technical Report FEMA-P-58-1, Washington, D.C., USA, 2012.

[22] E. Cosenza, C. Del Vecchio, M. Di Ludovico, M. Dolce, C. Moroni, A. Prota, E. Renzi, The Italian guidelines for seismic risk classification of constructions: technical principles and validation. *Bull. Earthq. Eng.*, **16,** 5905–5935, 2018.

[23] R. Gentile, C. Galasso, Simplicity versus accuracy trade-off in estimating seismic fragility of existing reinforced concrete buildings. *Soil Dyn. Earthq. Eng.*, **144**, 2021.

[24] S. Bianchi, J. Ciurlanti, S. Pampanin, A SLaMA-based analytical procedure for the Cost/Performance-based evaluation of buildings. *7th International Conference on Computational Methods in Structural Dynamics and Earthquake Engineering,* Crete, Greece, June 24-26, 2019.

[25] S. Bianchi, J. Ciurlanti, S. Pampanin, Comparison of traditional vs low-damage structural and non-structural building systems through a cost/performance-based evaluation. *Earthq. Spectra*. **37**, 366–385, 2021.

[26] D. D'Ayala, A. Meslem, D. Vamvatsikos, K. Porter, T. Rossetto, H. Crowley, V. Silva. *Guidelines for analytical vulnerability assessment - low/mid-rise*. GEM Technical Report, 2014.

[27] L. Martins, V. Silva, Development of a fragility and vulnerability model for global seismic risk analyses. *Bull. Earthq. Eng*., **19,** 6719–6745, 2021.

[28] R. Gentile, C. Galasso, Simplified seismic loss assessment for optimal structural retrofit of RC buildings. *Earthq. Spectra*, **37,** 346–365, 2021.

[29] Applied technology council. *Seismic evaluation and retrofit of concrete buildings*. ATC-40 report, Redwood City, CA, USA, 1996.

[30] P. Fajfar, A Nonlinear Analysis Method for Performance-Based Seismic Design. *Earthq. Spectra,* **16,** 573–592., 2000.

[31] G.J. O'Reilly, D. Perrone, M. Fox, R. Monteiro, A. Filiatrault, Seismic assessment and loss estimation of existing school buildings in Italy. *Eng. Struct*., **168**, 142–162, 2018.

[32] M. Dolce, G. Manfredi, Libro Bianco Sulla Ricostruzione Privata Fuori dai Centri Storici nei Comuni Colpiti dal Sisma Dell'abruzzo del 6 Aprile 2009. (In Italian). Doppiavoce, Napoli, Italy, 2016.

[33] D. Vamvatsikos, Accurate Application and Second-Order Improvement of SAC/FEMA Probabilistic Formats for Seismic Performance Assessment. *J. Struct. Eng.* **140,** 04013058, 2014.

[34] Italian Ministry of Infrastructures and Trasport. *Aggiornamento delle "Norme tecniche per le costruzioni"*. (in Italian). Supplemento ordinario n. 8 alla Gazzetta ufficiale del 20-2-2018, Rome, Italy, 2018.

[35] S. Pampanin, G.M. Calvi, M. Moratti, Seismic behaviour of RC beam-column joints designed for gravity loads. *12th European Conference on Earthquake Engineering,* London, UK, September 9-13, 2002.

[36] U. Akguzel, S. Pampanin, Assessment and design procedure for the seismic retrofit of reinforced concrete beam-column joints using FRP composite materials. *J. Compos. Constr.* **16**, 21–34, 2012.

[37] fib. Externally bonded FRP reinforcement for RC structures. fib bulletin 14. Lausanne, Switzerland, 2001.

[38] B, Lizundia, W.T. Holmes, K. Cobeen, J. Malley, H.S. Lew, Techniques for the seismic rehabilitation of existing buildings. *8th US National conference on earthquake engineering*, San Francisco, CA, US, April 18–22, 2006.

[39] M.J.N., Priestley, F. Seible, G.M. Calvi. *Seismic Design and Retrofit of Bridges*. New York: Wiley, 1996.

[40] S. Pampanin, Emerging Solutions for High Seismic Performance of Precast/Prestressed Concrete Buildings. *J. Adv. Concr. Technol* 3(2), 202-223, 2005.

[41] F. Sarti, A. Palermo, S. Pampanin, Fuse-type external replaceable dissipaters: experimental program and numerical modeling. *J Struct Eng*, **142(12)**, 04016134, 2016.

[42] fib. Seismic design of precast concrete structures. State-of-art report. fib bulletin 27. Lausanne, Switzerland, 2003.

[43] A. Cuevas, S. Pampanin, Post-Seismic Capacity of Damaged and Repaired Reinforced Concrete Plastic Hinges Extracted from a Real Building. 16th World Conference on Earthquake Engineering, Santiago Chile, January 9-1, 2017.

[44] D. Marriott, S. Pampanin, D. Bull, A. Palermo, Improving the seismic performance of existing reinforced concrete buildings using advanced rocking wall solutions. *New Zealand Society for Earthquake Engineering Conference*, Palmerston North, New Zealand, March 30–April 1, 2007.

[45] A.J., Carr, RUAUMOKO2D - The Maori God of Volcanoes and Earthquakes. Inelastic Analysis Finite Element program. Christchurch, New Zealand, 2016.

[46] M.J.N. Priestley, G.M. Calvi, M.J. Kowalsky, Displacement based seismic design of structures. Pavia: Iuss, Italy, 2007.

[47] S. Pampanin, G. Magenes, A. Carr, Modelling of shear hinge mechanism in poorly detailed RC beam–column joints. 4th fib Symposium, Athens, Greece, may 6-8, 2003.

[48] M. Saiidi, M.A. Sozen, *Simple and complex models for nonlinear seismic response of reinforced concrete structures*. Urbana, IL: University of Illinois at Urbana-Champaign, US, 1979.

[49] S. Pampanin, M.J.N. Priestley, S. Sritharan, Analytical modeling of the seismic behavior of precast concrete frames designed with ductile connections. *Journal of Earthquake Engineering*, **5(3)**, 329–367, 2001.

[50] M.P. Newcombe, S. Pampanin, A. Buchanan, A. Palermo, Section analysis and cyclic behavior of post-tensioned jointed ductile connections for multi-storey timber buildings. *Journal of Earthquake Engineering,* **12(S1)**, 83–110, 2008.

[51] F. Jalayer, R. De Risi, G. Manfredi, Bayesian Cloud Analysis: Efficient structural fragility assessment using linear regression. *Bull. Earthq. Eng.,* **13**, 1183–1203, 2015.

[52] F. Jalayer, H. Ebrahimian, A. Miano, G. Manfredi, H. Sezen, Analytical fragility assessment using unscaled ground motion records. *Earthq. Eng. Struct. Dyn.,* **46**, 2639–2663, 2017.

[53] C. Smerzini, C. Galasso, I. Iervolino, R. Paolucci, Ground motion record selection based on broadband spectral compatibility, *Earthquake Spectra*, **30(4)**, 1427–1448, 2014.

[54] C.B. Haselton, G.G. Deierlein, *Assessing seismic collapse safety of modern reinforced concrete moment-frame buildings*. Pacific Earthquake Engineering Center (PEER) 2007/08.

[55] R. Gentile, C. Galasso, Gaussian process regression for seismic fragility assessment of building portfolios. *Struct. Saf.* **87,** 2020.

[56] K. Aljawhari, R. Gentile, F. Freddi, C. Galasso, Effects of ground-motion sequences on fragility and vulnerability of case-study reinforced concrete frames. *Bull. Earthq. Eng.,* 2020.

[57] S. Lagomarsino, S. Giovinazzi, Macroseismic and mechanical models for the vulnerability and damage assessment of current buildings. *Bull. Earthq. Eng.,* **4**, 415–443, 2006.

[58] S. D'Amore, L. Pedone, S. Pampanin, Comparative analysis of code-compliant seismic assessment methods through nonlinear static analyses and demand spectrum: N2 Method vs. Capacity Spectrum Method. *Procedia Structural Integrity*, **44**, 378-385, 2023.

[59] S. D'Amore, S. Pampanin, Seismic Retrofit of Reinforced Concrete buildings using low-damage external exoskeletons. *2nd fib Italy YMG Symposium on concrete and concrete structures*, Rome, Italy, November 18-19, 2021.

[60] S. D'Amore, S. Pampanin, Enhancing seismic safety of existing RC buildings through external exoskeletons. *14th fib International PhD Symposium in Civil Engineering,* Rome, Italy, September 5-7, 2022.